IEEE Access
Multidisciplinary | Rapid Review | Open Access Journal

Received August 18, 2019, accepted August 27, 2019, date of publication September 2, 2019, date of current version September 17, 2019.

Digital Object Identifier 10.1109/ACCESS.2019.2938840

Discrete-Time ZND Models Solving ALRMPC via Eight-Instant General and Other Formulas of ZeaD

JIANRONG CHEN[1,2,3,4] AND YUNONG ZHANG[1,3,4], (Member, IEEE)

[1]School of Data and Computer Science, Sun Yat-sen University, Guangzhou 510006, China
[2]Information and Education Technology Center, Youjiang Medical University for Nationalities, Baise 533000, China
[3]Research Institute, Sun Yat-sen University, Shenzhen 518057, China
[4]Key Laboratory of Machine Intelligence and Advanced Computing, Ministry of Education, Sun Yat-sen University, Guangzhou 510006, China

Corresponding author: Yunong Zhang (zhynong@mail.sysu.edu.cn)

This work was supported in part by the National Natural Science Foundation of China under Grant 61976230, and in part by the Shenzhen Science and Technology Plan Project under Grant JCYJ20170818154936083.

ABSTRACT Repetitive motion planning and control (RMPC) of redundant robot manipulators is a fundamental and important problem widely existing in industrial manufacturing. In this paper, the acceleration-level RMPC (ALRMPC) is studied and solved in a discrete-time manner. For solving this problem, a new ALRMPC scheme with feedback control term is derived and presented at first. Then, by adopting Lagrange's undetermined multipliers method and zeroing neural dynamics (ZND), a continuous-time ZND model, which is based on the new ALRMPC scheme, is developed and proposed. Besides, an eight-instant general formula with high precision is constructed, proposed and analyzed. By using this eight-instant general formula and other multiple-instant Zhang et al discretization (ZeaD) formulas to discretize the continuous-time ZND model, four discrete-time ZND (DTZND) models for solving ALRMPC are thus obtained. Finally, theoretical analyses and computer simulation experiment results further substantiate the effectiveness and accuracy of the proposed DTZND models.

INDEX TERMS Acceleration-level repetitive motion planning and control (ALRMPC), zeroing neural dynamics (ZND), eight-instant general formula, redundant robot manipulators, quadratic programming (QP).

I. INTRODUCTION

With the development of artificial intelligence and industrial manufacturing, robotics technology has received unprecedented attention and extensive research [1]–[6]. As an important sub-topic of robotics, the repetitive motion planning and control (RMPC) of redundant robot manipulators has been investigated by a lot of researchers and experts, and many strategies and algorithms are proposed and applied [7]–[14]. One of the conventional strategies is the pseudo-inverse method [7]–[10], but it may introduce a divergence phenomenon in the tracking process of end-effector [11], [12]. Moreover, in the past ten years, quadratic programming (QP) method, which is widely used in the engineering and scientific fields, has been adopted by some scholars to describe RMPC schemes and solve them further [13], [14]. Since practical redundant robot manipulators are usually controlled by digital computer or system, exploiting some discrete-time models to solve RMPC, which is formulated in QP form, is necessary and meaningful.

For a time-varying problem like RMPC, both timeliness and accuracy must be considered. As an effective method, zeroing neural dynamics (ZND) has been applied to solve many time-varying problems, including RMPC, and good results have been achieved [15]–[19]. Generally, for a continuous-time ZND model, we can use a valid one-step-ahead discretization formula to discretize it and obtain a corresponding discrete-time ZND (DTZND) model. Note that the accuracy of the obtained discrete-time solving models is closely related to the used discretization formulas. Specifically, high precision discretization formulas correspond to high precision discrete models, and vice versa [20]–[24]. Therefore, in order to obtain high precision DTZND model, a general form of eight-instant Zhang et al discretization (ZeaD) formula is derived, proposed and investigated.

The associate editor coordinating the review of this article and approving it for publication was Jinguo Liu.

This paper is mainly concerned with applying the ZND method to solve acceleration-level RMPC (ALRMPC) problem in a discrete-time manner. The rest of this paper is organized into four sections. A new ALRMPC scheme and the corresponding continuous-time ZND model are developed in Section II. In Section III, the eight-instant general formula is proposed, and four DTZND models, i.e., two-instant DTZND (TIDTZND), four-instant DTZND (FIDTZND), six-instant DTZND (SIDTZND), and eight-instant DTZND (EIDTZND) models, are further derived and investigated. Section IV shows the numerical experiments and verifications, and Section V concludes this paper with final remarks. Before ending this section, the main contributions of this work are listed as below.

1) A new ALRMPC scheme is derived, presented and investigated in this paper. Besides, by employing ZND, a continuous-time ZND model for solving ALRMPC is further developed and proposed.
2) A novel high precision eight-instant general formula is constructed and proposed with corresponding theoretical analyses.
3) For digital hardware realization, by exploiting the eight-instant general formula and other multiple-instant ZeaD formulas, four DTZND models, with $O(\tau^2)$, $O(\tau^3)$, $O(\tau^4)$, and $O(\tau^5)$ precision respectively, are proposed and discussed.
4) Theoretical analyses and numerical experiment results indicate that the proposed DTZND models are effective and feasible for solving ALRMPC.

II. ACCELERATION-LEVEL RMPC SCHEME

As a basis for further discussion, the new ALRMPC scheme and the corresponding continuous-time ZND model are presented and investigated in this section.

A. NEW ALRMPC SCHEME DESIGN

In the previous work [25], [26], the redundancy resolution problem of redundant robot manipulators at the acceleration level can be formulated as follows:

$$\begin{aligned}&\text{min.}\ \frac{1}{2}(\ddot{\theta}(t)+\mathbf{c}(t))^{\mathrm{T}}(\ddot{\theta}(t)+\mathbf{c}(t)),\\&\text{s. t.}\ J(\theta(t))\ddot{\theta}(t)=\ddot{\mathbf{r}}_{\mathrm{a}}(t),\end{aligned}$$

where $\mathbf{c}(t) = (u_1+u_2)\dot{\theta}(t)+u_1u_2(\theta(t)-\theta(0))$, $\ddot{\mathbf{r}}_{\mathrm{a}}(t) = \ddot{\mathbf{r}}_{\mathrm{d}}(t)-\dot{J}(\theta(t))\dot{\theta}(t)$; $\theta(t)\in\mathbb{R}^n$, $\dot{\theta}(t)\in\mathbb{R}^n$ and $\ddot{\theta}(t)\in\mathbb{R}^n$ denote joint-angle vector, joint-velocity vector and joint-acceleration vector, respectively; $\theta(0)$ denotes the initial value of joint-angle vector $\theta(t)$; $u_1, u_2\in\mathbb{R}^+$ are design parameters; $\mathbf{r}_{\mathrm{d}}(t)\in\mathbb{R}^m$ is a given desired end-effector path and $\ddot{\mathbf{r}}_{\mathrm{d}}(t)$ is the second order time derivative of $\mathbf{r}_{\mathrm{d}}(t)$; $J(\theta(t)) = \partial f(\theta(t))/\partial\theta(t)\in\mathbb{R}^{m\times n}$ is the Jacobian matrix, and $f(\theta(t))\in\mathbb{R}^m$ denotes a differentiable nonlinear function with the structure and parameters known for a given redundant robot manipulator; $\dot{J}(\theta(t))$ denotes the time derivative of Jacobian matrix $J(\theta(t))$.

Note that the obtained joint-angle vector $\theta(t)$ can not strictly make $\mathbf{r}_{\mathrm{d}}(t)-f(\theta(t)) = 0$, because the disturbance and computational round-off errors always exist in practical application. Therefore, a feedback control term is derived and presented here to handle this situation, which is different from the one introduced in [25]. To obtain the feedback control term, we define two vector-valued error functions consecutively and use ZND linear design formula [i.e., $\dot{\mathbf{e}}(t) = -\mu\mathbf{e}(t)$] twice, with the detailed design process as follows.

We define the first vector-valued error function as

$$\mathbf{e}_1(t) = \mathbf{r}_{\mathrm{d}}(t)-f(\theta(t)).$$

Then, by making use of the ZND linear design formula, we have

$$\dot{\mathbf{r}}_{\mathrm{d}}(t)-J(\theta(t))\dot{\theta}(t) = -\mu_1(\mathbf{r}_{\mathrm{d}}(t)-f(\theta(t))),$$

that is,

$$\dot{\mathbf{r}}_{\mathrm{d}}(t)-J(\theta(t))\dot{\theta}(t)+\mu_1(\mathbf{r}_{\mathrm{d}}(t)-f(\theta(t))) = 0.$$

The second vector-valued error function is defined as

$$\mathbf{e}_2(t) = \dot{\mathbf{r}}_{\mathrm{d}}(t)-J(\theta(t))\dot{\theta}(t)+\mu_1(\mathbf{r}_{\mathrm{d}}(t)-f(\theta(t))).$$

By adopting the linear design formula again, we have

$$\begin{aligned}&\ddot{\mathbf{r}}_{\mathrm{d}}(t)-\dot{J}(\theta(t))\dot{\theta}(t)-J(\theta(t))\ddot{\theta}(t)+\mu_1(\dot{\mathbf{r}}_{\mathrm{d}}(t)-J(\theta(t))\dot{\theta}(t))\\&\quad = -\mu_2(\dot{r}_{\mathrm{d}}(t)-J(\theta(t))\dot{\theta}(t)+\mu_1(\mathbf{r}_{\mathrm{d}}(t)-f(\theta(t)))),\end{aligned}$$

and further have

$$\begin{aligned}&J(\theta(t))\ddot{\theta}(t)\\&\quad = \ddot{\mathbf{r}}_{\mathrm{d}}(t)-\dot{J}(\theta(t))\dot{\theta}(t)+\mu_1(\dot{\mathbf{r}}_{\mathrm{d}}(t)-J(\theta(t))\dot{\theta}(t))\\&\qquad +\mu_2(\dot{\mathbf{r}}_{\mathrm{d}}(t)-J(\theta(t))\dot{\theta}(t)+\mu_1(\mathbf{r}_{\mathrm{d}}(t)-f(\theta(t)))).\end{aligned}$$

After arranging, the feedback control term is thus formulated as below:

$$\begin{aligned}\mathbf{r}_{\mathrm{fb}}(t) = (\mu_1+\mu_2)(\dot{\mathbf{r}}_{\mathrm{d}}(t)-J(\theta(t))\dot{\theta}(t))\\+\mu_1\mu_2(\mathbf{r}_{\mathrm{d}}(t)-f(\theta(t))).\end{aligned}$$

Note that the design parameters μ_1 and μ_2 are positive real numbers.

As a result, the new ALRMPC scheme is given by the following theorem.

Theorem 1: With $\mathbf{r}_{\mathrm{fb}}(t)$ denoting the feedback control term, and the other symbols are defined as before, the new ALRMPC scheme of redundant robot manipulators can be described as below:

$$\text{min.}\ \frac{1}{2}(\ddot{\theta}(t)+\mathbf{c}(t))^{\mathrm{T}}(\ddot{\theta}(t)+\mathbf{c}(t)), \tag{1}$$

$$\text{s. t.}\ J(\theta(t))\ddot{\theta}(t) = \ddot{\mathbf{r}}_{\mathrm{a}}(t)+\mathbf{r}_{\mathrm{fb}}(t). \tag{2}$$

Proof: The detailed proof process of (1) can be generalized from [25]. In addition, from the previous derivation we get (2). The proof is thus completed. ■

B. CONTINUOUS-TIME ZND MODEL

To solve (1)-(2), we first transform it into an equivalent standard QP problem as below:

$$\begin{aligned}&\text{min.}\ \ \frac{1}{2}\mathbf{x}^{\mathrm{T}}(t)A(t)\mathbf{x}(t)+\mathbf{c}^{\mathrm{T}}(t)\mathbf{x}(t),\\&\text{s. t.}\ \ B(t)\mathbf{x}(t)=\mathbf{d}(t),\end{aligned}$$

where $\mathbf{x}(t) = \ddot{\theta}(t)$, $A(t) = I$, $B(t) = J(\theta(t))$, $\mathbf{d}(t) = \ddot{\mathbf{r}}_{\mathrm{a}}(t) + \mathbf{r}_{\mathrm{fb}}(t)$, and $\mathbf{c}(t)$ is defined as before. Evidently, it can be simplified and reformulated immediately as

$$\text{min.}\ \ \frac{1}{2}\mathbf{x}^{\mathrm{T}}(t)\mathbf{x}(t)+\mathbf{c}^{\mathrm{T}}(t)\mathbf{x}(t), \tag{3}$$

$$\text{s. t.}\ \ B(t)\mathbf{x}(t)=\mathbf{d}(t). \tag{4}$$

Besides, according to the method of Lagrange's undetermined multipliers [27], [28], we define a Lagrange function

$$L(\mathbf{x}(t),\lambda(t)) = \frac{1}{2}\mathbf{x}^{\mathrm{T}}(t)\mathbf{x}(t)+\mathbf{c}^{\mathrm{T}}(t)\mathbf{x}(t) + \lambda^{\mathrm{T}}(t)(B(t)\mathbf{x}(t)-\mathbf{d}(t)),$$

where $\lambda(t) \in \mathbb{R}^m$ denotes the Lagrange-multiplier vector. Then, we have the following equations:

$$\begin{cases}\dfrac{\partial L(\mathbf{x}(t),\lambda(t))}{\partial \mathbf{x}(t)} = \mathbf{x}(t)+\mathbf{c}(t)+B^{\mathrm{T}}(t)\lambda(t)=0,\\ \dfrac{\partial L(\mathbf{x}(t),\lambda(t))}{\partial \lambda(t)} = B(t)\mathbf{x}(t)-\mathbf{d}(t)=0,\end{cases}$$

which can be rewritten in a compact form as

$$F(t)\mathbf{z}(t)+\mathbf{w}(t)=0, \tag{5}$$

where $F(t) = [I, B^{\mathrm{T}}(t); B(t), 0] \in \mathbb{R}^{(n+m)\times(n+m)}$, $\mathbf{z}(t) = [\mathbf{x}(t); \lambda(t)] \in \mathbb{R}^{n+m}$ and $\mathbf{w}(t) = [\mathbf{c}(t); -\mathbf{d}(t)] \in \mathbb{R}^{n+m}$. Since the identity matrix I is positive definite and $B(t)$ is of full row rank, $F(t)$ is nonsingular at any time instant $t \in [t_0, t_{\mathrm{f}}) \subseteq [0, +\infty)$, which guarantees the solution uniqueness of (5).

Furthermore, by applying the ZND method, a vector-valued error function is defined as $\mathbf{e} = F(t)\mathbf{z}(t) + \mathbf{w}(t)$, and then the linear design formula [i.e., $\dot{\mathbf{e}}(t) = -v\mathbf{e}(t)$] is employed to force this error function to converge to zero. Finally, the continuous-time ZND model for solving ALRMPC is obtained as follows:

$$\dot{\mathbf{z}}(t) = -F^{-1}(t)((\dot{F}(t)+vF(t))\mathbf{z}(t)+\dot{\mathbf{w}}(t)+v\mathbf{w}(t)), \tag{6}$$

where $v \in \mathbb{R}^+$ is the design parameter and $F^{-1}(t)$ is the inverse of $F(t)$; $\dot{\mathbf{z}}(t)$ and $\dot{F}(t)$ denote the time derivative of $\mathbf{z}(t)$ and $F(t)$, respectively.

III. DISCRETE-TIME ZND MODELS FOR ALRMPC SOLVING

In this section, four discrete-time ZND models with different precision are proposed, developed and investigated. Besides, the corresponding theoretical analyses are also provided.

A. EIGHT-INSTANT GENERAL FORMULA

The eight-instant general formula is proposed by the following theorem.

Theorem 2: With $\tau \in (0, 1)$ denoting the sampling gap, and η_1, η_2, and η_3 are real numbers which satisfy

$$\begin{cases}2\eta_1-24\eta_2-25\eta_3>7,\\ 10\eta_1+8\eta_2+13\eta_3>-15,\\ 10\eta_1+8\eta_2+3\eta_3<35,\\ 530\eta_1+712\eta_2+387\eta_3<-245,\\ 29900\eta_1^2+98720\eta_1\eta_2+61720\eta_1\eta_3\\ +99200\eta_1+73664\eta_2^2+86528\eta_2\eta_3\\ +102880\eta_2+24489\eta_3^2+36130\eta_3<-21525,\\ 47800\eta_1^3-134160\eta_1^2\eta_2-191060\eta_1^2\eta_3-49900\eta_1^2\\ -784512\eta_1\eta_2^2-1347344\eta_1\eta_2\eta_3-1148080\eta_1\eta_2\\ -546582\eta_1\eta_3^2-1165780\eta_1\eta_3-387350\eta_1\\ -649984\eta_2^3-1441856\eta_2^2\eta_3-1148608\eta_2^2\\ -1020660\eta_2\eta_3^2-1597496\eta_2\eta_3-578260\eta_2\\ -228663\eta_3^3-410763\eta_3^2-329285\eta_3<82425,\end{cases} \tag{7}$$

the general form of eight-instant ZeaD formula is formulated as below:

$$\dot{f}_k = b_0(f_{k+1}+b_1f_k+\eta_1f_{k-1}+\eta_2f_{k-2}+\eta_3f_{k-3} + \eta_4f_{k-4}+\eta_5f_{k-5}+\eta_6f_{k-6})/\tau+O(\tau^4), \tag{8}$$

where $b_0 = 20/(35-10\eta_1-8\eta_2-3\eta_3)$, $b_1 = -(805+970\eta_1+536\eta_2+171\eta_3)/1200$, $\eta_4 = -(21+10\eta_1+24\eta_2+27\eta_3)/16$, $\eta_5 = (35+15\eta_1+32\eta_2+27\eta_3)/25$, and $\eta_6 = -(5+2\eta_1+4\eta_2+3\eta_3)/12$.

Proof: The proof process is given in Appendix B. ■

For the convenience of readers and researchers, the effective range of parameters η_1, η_2, and η_3 is shown in Fig. 1 intuitively. In addition, the collection of eight-instant ZeaD formulas with different parameter values is shown in Table 1.

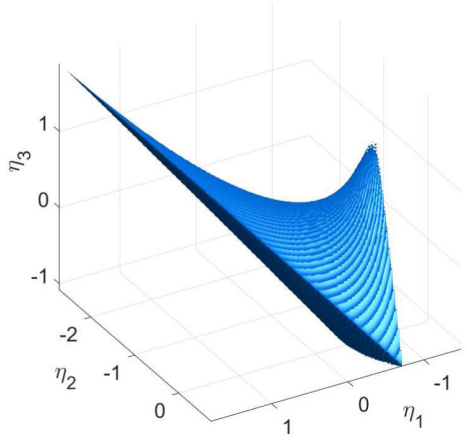

FIGURE 1. Effective range composed of parameters η_1, η_2, and η_3 in eight-instant general ZeaD formula.

TABLE 1. Collection of eight-instant ZeaD formulas with different values of η_1, η_2, and η_3.

η_1	η_2	η_3	Eight-instant ZeaD formula
0.4	−1.2	0.5	$\dot{f}_k = (\frac{200}{391}f_{k+1} - \frac{6353}{23460}f_k + \frac{80}{391}f_{k-1} - \frac{240}{391}f_{k-2} + \frac{100}{391}f_{k-3} - \frac{485}{1564}f_{k-4} + \frac{28}{85}f_{k-5} - \frac{125}{1173}f_{k-6})/\tau + O(\tau^4)$
−0.7	0.4	−0.8	$\dot{f}_k = (\frac{50}{103}f_{k+1} - \frac{509}{6180}f_k - \frac{35}{103}f_{k-1} + \frac{20}{103}f_{k-2} - \frac{40}{103}f_{k-3} - \frac{25}{412}f_{k-4} + \frac{157}{515}f_{k-5} - \frac{35}{309}f_{k-6})/\tau + O(\tau^4)$
−0.8	−0.7	0.1	$\dot{f}_k = (\frac{200}{483}f_{k+1} + \frac{1097}{9660}f_k - \frac{160}{483}f_{k-1} - \frac{20}{69}f_{k-2} + \frac{20}{483}f_{k-3} + \frac{55}{1932}f_{k-4} + \frac{44}{805}f_{k-5} - \frac{5}{161}f_{k-6})/\tau + O(\tau^4)$
0.4	−1	0.4	$\dot{f}_k = (\frac{100}{189}f_{k+1} - \frac{403}{1260}f_k + \frac{40}{189}f_{k-1} - \frac{100}{189}f_{k-2} + \frac{40}{189}f_{k-3} - \frac{295}{756}f_{k-4} + \frac{44}{105}f_{k-5} - \frac{25}{189}f_{k-6})/\tau + O(\tau^4)$
−0.2	−0.8	0.2	$\dot{f}_k = (\frac{50}{107}f_{k+1} - \frac{541}{6420}f_k - \frac{10}{107}f_{k-1} - \frac{40}{107}f_{k-2} + \frac{10}{107}f_{k-3} - \frac{65}{428}f_{k-4} + \frac{118}{535}f_{k-5} - \frac{25}{321}f_{k-6})/\tau + O(\tau^4)$
0.6	−1.4	0.7	$\dot{f}_k = (\frac{200}{381}f_{k+1} - \frac{2521}{7620}f_k + \frac{40}{127}f_{k-1} - \frac{280}{381}f_{k-2} + \frac{140}{381}f_{k-3} - \frac{205}{508}f_{k-4} + \frac{724}{1905}f_{k-5} - \frac{15}{127}f_{k-6})/\tau + O(\tau^4)$
−0.3	0.2	−0.6	$\dot{f}_k = (\frac{100}{191}f_{k+1} - \frac{2593}{11460}f_k - \frac{30}{191}f_{k-1} + \frac{20}{191}f_{k-2} - \frac{60}{191}f_{k-3} - \frac{165}{764}f_{k-4} + \frac{414}{955}f_{k-5} - \frac{85}{573}f_{k-6})/\tau + O(\tau^4)$

B. FOUR DTZND MODELS FOR ALRMPC

For the purpose of digital hardware realization, four DTZND models for solving ALRMPC (6) are proposed, discussed and studied.

By using (8) to discretize (6), the general EIDTZND model is obtained as follows:

$$\begin{aligned}\mathbf{z}_{k+1} = \widetilde{\mathbf{z}}_k/b_0 - b_1\mathbf{z}_k - \eta_1\mathbf{z}_{k-1} - \eta_2\mathbf{z}_{k-2} - \eta_3\mathbf{z}_{k-3} \\ - \eta_4\mathbf{z}_{k-4} - \eta_5\mathbf{z}_{k-5} - \eta_6\mathbf{z}_{k-6} + \mathbf{O}(\tau^5),\end{aligned} \tag{9}$$

with

$$\widetilde{\mathbf{z}}_k = -F_k^{-1}((\tau\dot{F}_k + hF_k)\mathbf{z}_k + \tau\dot{\mathbf{w}}_k + h\mathbf{w}_k),$$

in which $h = \tau v$; F_k, $\mathbf{z}_k$ and $\mathbf{w}_k$ denote $F(t_k)$, $\mathbf{z}(t_k)$ and $\mathbf{w}(t_k)$, respectively.

Theorem 3: With $\tau \in (0, 1)$ denoting the sampling gap, symbol $||\cdot||_2$ denoting the Euclidean-norm of a vector and $\mathbf{O}(\tau^5)$ denoting a vector with every entry being $O(\tau^5)$, the general EIDTZND model (9) is 0-stable, consistent and convergent, which converges with the order of its truncation error being $\mathbf{O}(\tau^5)$. Moreover, the maximal steady-state residual error $\limsup_{k\to+\infty}||F_{k+1}\mathbf{z}_{k+1} + \mathbf{w}_{k+1}||_2$ of (9) is $O(\tau^5)$.

Proof: According to Result 1 in Appendix A and the proof process of Theorem 2 in Appendix B, the general EIDTZND model (9) discretized by eight-instant general ZeaD formula (8) in the effective range is 0-stable. Evidently, according to Result 2 in Appendix A, the general EIDTZND model (9) is consistent. Besides, according to Results 3 and 4 in Appendix A, (9) is convergent and it converges with the order of its truncation error $\mathbf{O}(\tau^5)$.

Assume $\mathbf{z}^*_{k+1}$ is the theoretical solution of $F_{k+1}\mathbf{z}_{k+1} + \mathbf{w}_{k+1} = \mathbf{0}$. In addition, we have $\mathbf{z}_{k+1} = \mathbf{z}^*_{k+1} + \mathbf{O}(\tau^5)$ with k being large enough.

$$\begin{aligned}&\limsup_{k\to+\infty}||F_{k+1}\mathbf{z}_{k+1} + \mathbf{w}_{k+1}||_2 \\ &\quad= \limsup_{k\to+\infty}||F_{k+1}(\mathbf{z}^*_{k+1} + \mathbf{O}(\tau^5)) + \mathbf{w}_{k+1}||_2 \\ &\quad= \limsup_{k\to+\infty}||F_{k+1}\mathbf{z}^*_{k+1} + \mathbf{w}_{k+1} + F_{k+1}\mathbf{O}(\tau^5)||_2 \\ &\quad= \limsup_{k\to+\infty}||F_{k+1}\mathbf{O}(\tau^5)||_2 = O(\tau^5).\end{aligned}$$

This completes the proof. ■

Furthermore, in order to obtain other DTZND models, three ZeaD formulas with different precision are adopted. The first one is Euler forward formula [29], which can be seen as the first and also the simplest one of ZeaD formulas:

$$\dot{f}_k = \frac{f_{k+1} - f_k}{\tau} + O(\tau).$$

The second one is the four-instant ZeaD (specifically, Taylor-type) formula [23]:

$$\dot{f}_k = \frac{2f_{k+1} - 3f_k + 2f_{k-1} - f_{k-2}}{2\tau} + O(\tau^2).$$

The third one is the six-instant ZeaD formula [24]:

$$\dot{f}_k = \frac{24f_{k+1} - 5f_k - 12f_{k-1} - 6f_{k-2} - 4f_{k-3} + 3f_{k-4}}{48\tau} + O(\tau^3).$$

Similarly, by using them to discretize (6) respectively, the corresponding DTZND models are obtained as

$$\mathbf{z}_{k+1} = \widetilde{\mathbf{z}}_k + \mathbf{z}_k + \mathbf{O}(\tau^2), \tag{10}$$

$$\mathbf{z}_{k+1} = \widetilde{\mathbf{z}}_k + \frac{3}{2}\mathbf{z}_k - \mathbf{z}_{k-1} + \frac{1}{2}\mathbf{z}_{k-2} + \mathbf{O}(\tau^3), \tag{11}$$

and

$$\begin{aligned}\mathbf{z}_{k+1} = 2\widetilde{\mathbf{z}}_k + \frac{5}{24}\mathbf{z}_k + \frac{1}{2}\mathbf{z}_{k-1} + \frac{1}{4}\mathbf{z}_{k-2} \\ + \frac{1}{6}\mathbf{z}_{k-3} - \frac{1}{8}\mathbf{z}_{k-4} + \mathbf{O}(\tau^4),\end{aligned} \tag{12}$$

which are termed two-instant DTZND (TIDTZND) model, four-instant DTZND (FIDTZND) model, and six-instant DTZND (SIDTZND) model, respectively. Note that the definition of $\widetilde{\mathbf{z}}_k$ is consistent with that of EIDTZND model (9).

Theorem 4: With $\tau \in (0, 1)$ denoting the sampling gap, the TIDTZND (10), FIDTZND (11) and SIDTZND (12) models are 0-stable, consistent and convergent, which converge with the order of the truncation error being $\mathbf{O}(\tau^2)$, $\mathbf{O}(\tau^3)$, and $\mathbf{O}(\tau^4)$, respectively. Moreover, the maximal steady-state residual errors $\limsup_{k\to+\infty}||F_{k+1}\mathbf{z}_{k+1} + \mathbf{w}_{k+1}||_2$ of (10), (11) and (12) are $O(\tau^2)$, $O(\tau^3)$, and $O(\tau^4)$, respectively.

Proof: It is omitted because of its similarity to that of Theorem 3. ■

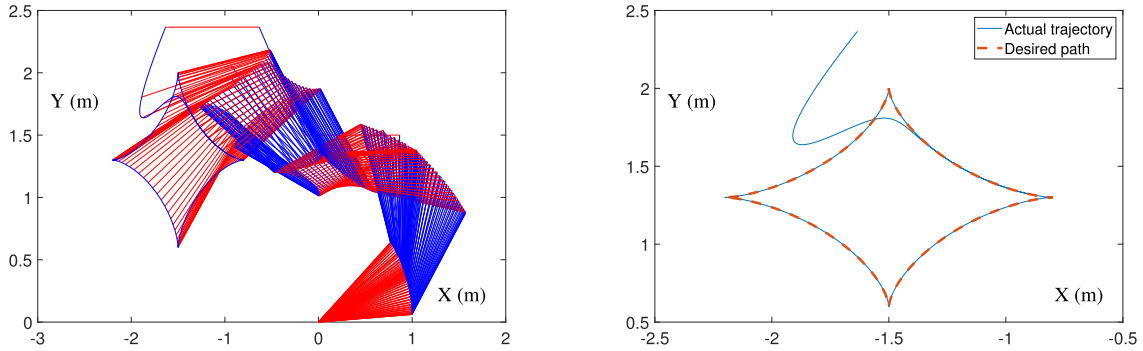

(a) Robot manipulator motion (b) End-effector trajectory

FIGURE 2. Simulation motion and trajectory synthesized by EIDTZND (9) for the 5-link planar manipulator tracking the astroid path.

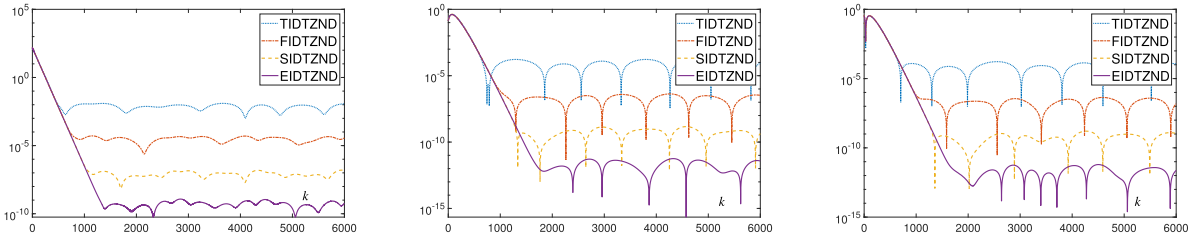

(a) Residual errors of different DTZND models (b) Tracking errors of X-axis (c) Tracking errors of Y-axis

FIGURE 3. Residual and tracking errors synthesized by different DTZND models for the 5-link planar manipulator tracking the astroid path (Unit: m).

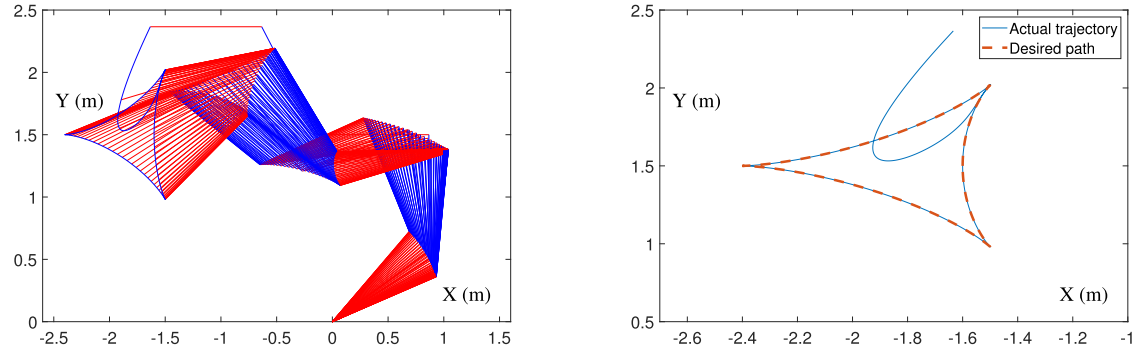

(a) Robot manipulator motion (b) End-effector trajectory

FIGURE 4. Simulation motion and trajectory synthesized by EIDTZND (9) for the 5-link planar manipulator tracking the tricuspid path.

IV. NUMERICAL EXPERIMENTS AND VERIFICATIONS

Based on the previous analyses, to substantiate the effectiveness of DTZND models, i.e., TIDTZND (10), FIDTZND (11), SIDTZND (12), and EIDTZND (9) models, for solving ALRMPC, computer simulation experiments are conducted in this section. Specifically, the real-time motion control of a 5-link planar redundant robot manipulator and a 3-dimension redundant robot manipulator (e.g., the PUMA560 robot manipulator [30]) is simulated, performed and investigated.

For the purposes of simplification, the parameters are uniformly set as $u_1 = u_2 = \mu_1 = \mu_2 = 10$, $\tau = 0.002$ s and $h = 0.02$. In addition, the parameters η_1, η_2, and η_3 of EIDTZND (9) are set as -0.8, -0.7, and 0.1, respectively.

Note that, in all simulation experiments, we investigate the residual error $||F_{k+1}\mathbf{z}_{k+1}+\mathbf{w}_{k+1}||_2$ and tracking error to scale the computational accuracy of different models, respectively.

A. 5-LINK PLANAR REDUNDANT ROBOT MANIPULATOR

In this subsection, the proposed four DTZND models are simulated on the 5-link planar manipulator with its

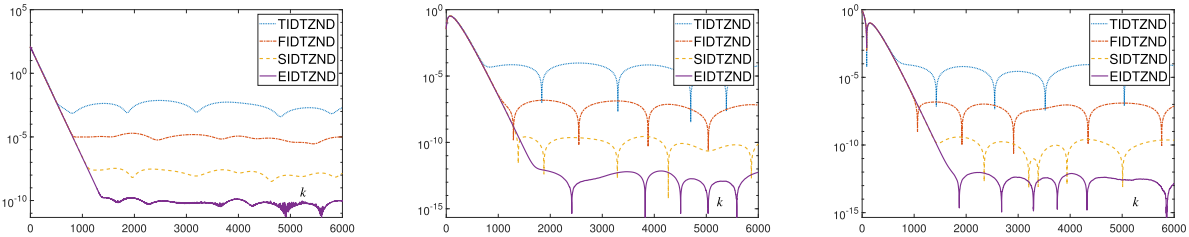

(a) Residual errors of different DTZND models (b) Tracking errors of X-axis (c) Tracking errors of Y-axis

FIGURE 5. Residual and tracking errors synthesized by different DTZND models for the 5-link planar manipulator tracking the tricuspid path (Unit: m).

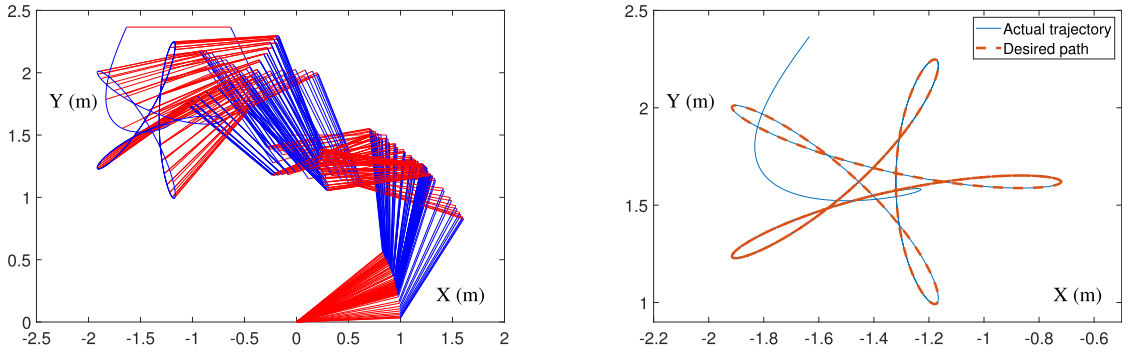

(a) Robot manipulator motion (b) End-effector trajectory

FIGURE 6. Simulation motion and trajectory synthesized by EIDTZND (9) for the 5-link planar manipulator tracking the inner five rings path.

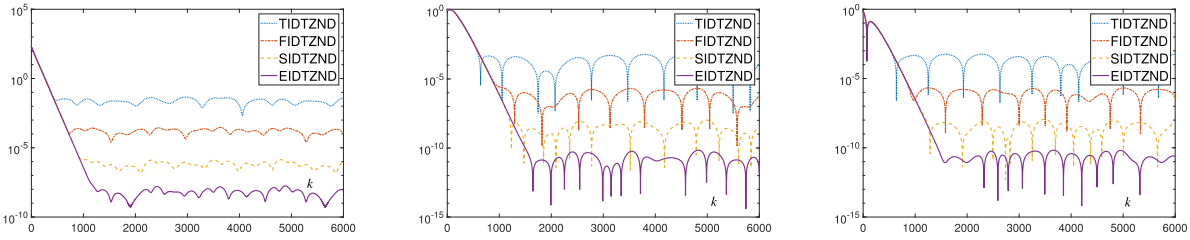

(a) Residual errors of different DTZND models (b) Tracking errors of X-axis (c) Tracking errors of Y-axis

FIGURE 7. Residual and tracking errors synthesized by different DTZND models for the 5-link planar manipulator tracking the inner five rings path (Unit: m).

end-effector tracking an astroid path, a tricuspid path and an inner five rings path, respectively. Besides, the initial joint state of the robot manipulator is set as $\theta(0) = [\pi/6; \pi/3; \pi/2; -\pi/3; \pi/3]$ rad and the duration of the path tracking task is set as $t_f = 12$ s in each experiment uniformly.

The motion trajectories of robot manipulator and the end-effector trajectories synthesized by EIDTZND (9) in tracking the astroid path, the tricuspid path and the inner five rings path are shown in Figs. 2, 4, and 6, respectively, and those synthesized by TIDTZND (10), FIDTZND (11) and SIDTZND (12) are omitted because of similarity and space limitation. As shown in these figures, each actual tracking path coincides with the corresponding desired path, which substantiates the proposed DTZND models for ALRMPC are correct and feasible. In addition, from Figs. 3(a), 5(a), and 7(a), we can see that the residual errors synthesized by models (10), (11), (12), and (9) change regularly, which are in accordance with Theorems 3 and 4. Furthermore, in Figs. 3(b), 3(c), 5(b), 5(c), 7(b), and 7(c), the tracking errors of X-axis and Y-axis for (10), (11), (12), and (9) also change regularly. Thus, the efficacy of DTZND models is substantiated.

B. 3-DIMENSION REDUNDANT ROBOT MANIPULATOR

For further substantiating the effectiveness of the proposed four DTZND models for ALRMPC, we conduct the computer simulation experiments on the 3-dimension manipulator with its end-effector tracking a ring-like conic path and a

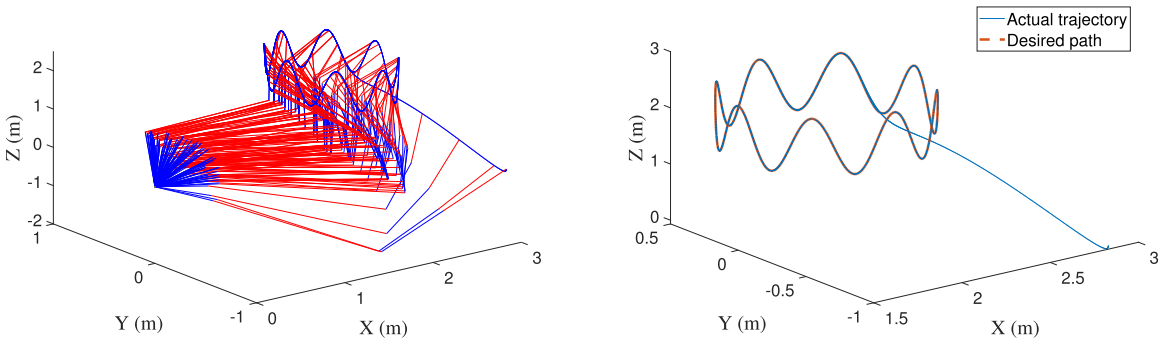

(a) Robot manipulator motion (b) End-effector trajectory

FIGURE 8. Simulation motion and trajectory synthesized by EIDTZND (9) for the 3-dimension manipulator tracking the ring-like conic path.

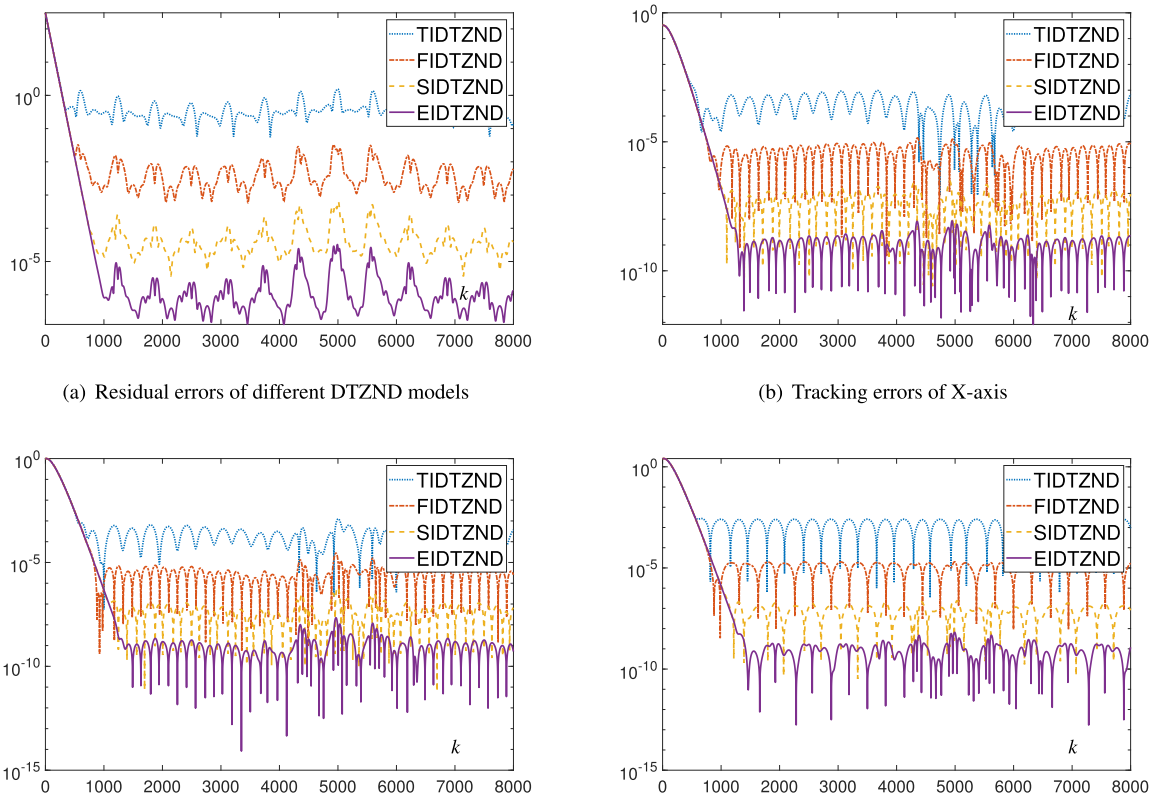

(a) Residual errors of different DTZND models (b) Tracking errors of X-axis

(c) Tracking errors of Y-axis (d) Tracking errors of Z-axis

FIGURE 9. Residual and tracking errors synthesized by different DTZND models for the 3-dimension manipulator tracking the ring-like conic path (Unit: m).

ring spiral path. Moreover, in the simulation experiments, the initial joint state of the robot manipulator is consistently set as $\theta(0) = [0; -\pi/4; 0; \pi/2; 0; -\pi/4]$ rad, and the durations of the path tracking task are respectively set as 16 s and 14 s.

Because of similarity and space limitation, only the motion and the end-effector trajectories of robot manipulator synthesized by EIDTZND (9) in tracking the ring-like conic path and the ring spiral path are given in Figs. 8 and 10. As seen in these two figures, the actual tracking paths and the desired paths are overlapped, which substantiates the correctness of the proposed DTZND models for ALRMPC. Besides, as shown in Figs. 9(a) and 11(a), it is evident that the residual errors of (10), (11), (12), and (9) are increased successively, which coincide with Theorems 3 and 4. From Figs. 9(b) through 9(d) and 11(b) through 11(d), we know that the tracking errors of different DTZND models are also increased successively. These results show that the proposed DTZND models are effective and feasible.

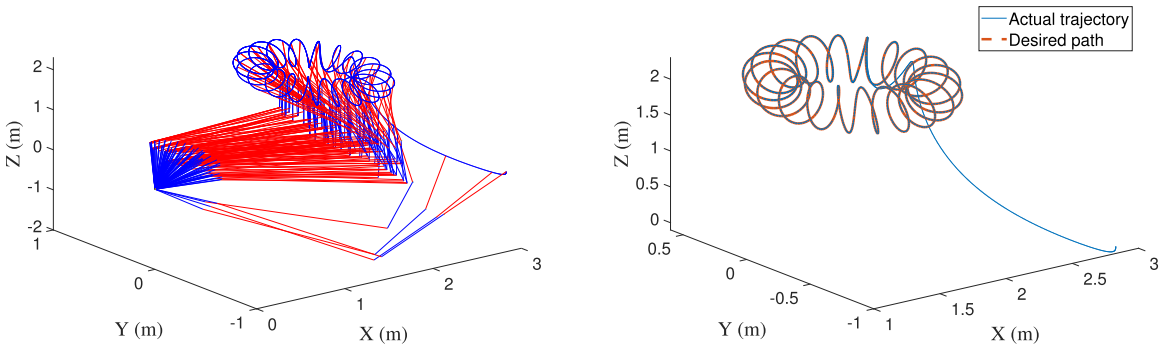

(a) Robot manipulator motion (b) End-effector trajectory

FIGURE 10. Simulation motion and trajectory synthesized by EIDTZND (9) for the 3-dimension manipulator tracking the ring spiral path.

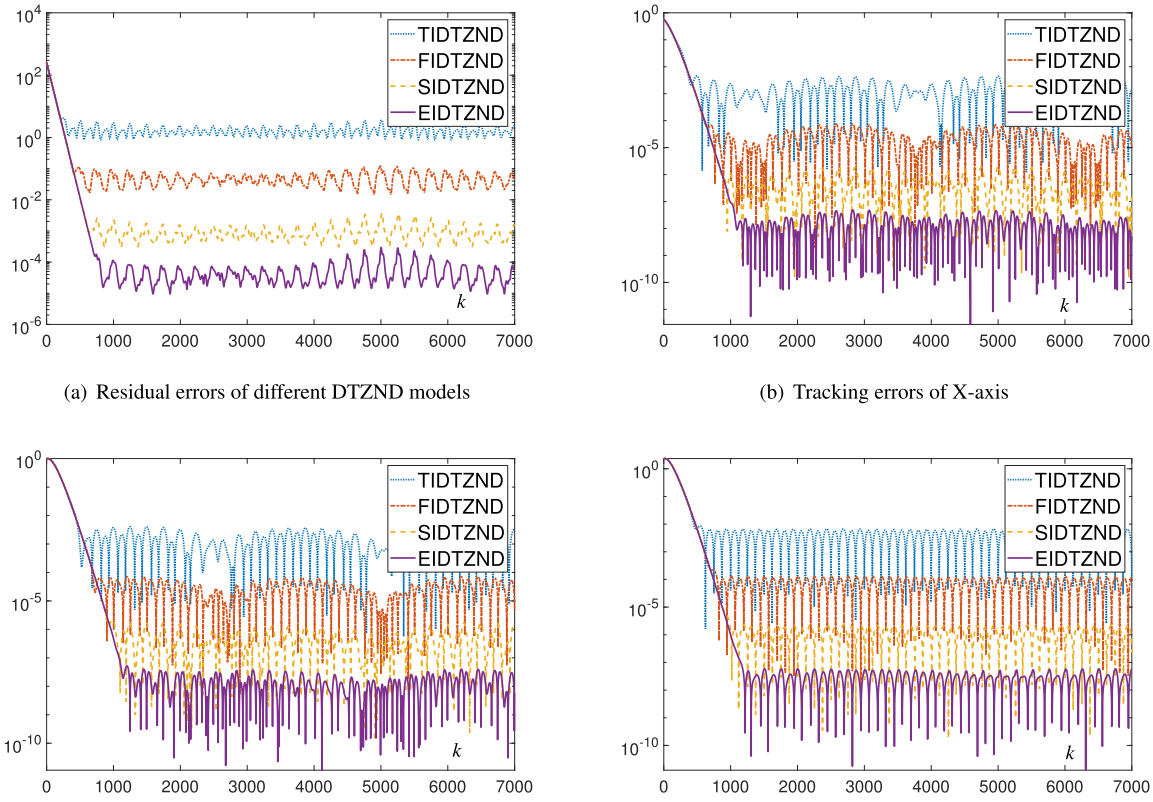

(a) Residual errors of different DTZND models (b) Tracking errors of X-axis

(c) Tracking errors of Y-axis (d) Tracking errors of Z-axis

FIGURE 11. Residual and tracking errors synthesized by different DTZND models for the 3-dimension manipulator tracking the ring spiral path (Unit: m).

V. CONCLUSION

In this work, the ALRMPC problem has been investigated, and then solved by the proposed DTZND models successfully. Specifically, the new ALRMPC scheme has been presented and investigated. Then, the corresponding continuous-time ZND model has been developed and proposed by applying the ZND method. Furthermore, the eight-instant general formula has been proposed and studied. Based on the eight-instant general formula and other ZeaD formulas, four DTZND models with different precision have been further derived and proposed. Finally, theoretical analyses and numerical experiment results have indicated the good effectiveness and superiority of the proposed DTZND models. As an extension of this work, one of the future research topics is to study and analyze the effective step-size interval of different DTZND models. Besides, constructing and finding new multiple-instant general ZeaD formulas with higher precision can also be an interesting research direction.

APPENDIX A

In Appendix A, the following four results [29], [31] for a linear N-step method are provided.

Result 1: A linear N-step method $\sum_{i=0}^{N}\alpha_i x_{k+i} = \tau\sum_{i=0}^{N}\kappa_i\psi_{k+i}$ can be checked for 0-stability by determining the roots of its characteristic polynomial $P_N(\varsigma)=\sum_{i=0}^{N}\alpha_i\varsigma^i$. If all roots denoted by ς of the polynomial $P_N(\varsigma)$ satisfy $|\varsigma|\leq 1$ with $|\varsigma|=1$ being simple, then the linear N-step method is 0-stable (i.e., has 0-stability).

Result 2: A linear N-step method is said to be consistent (i.e., have consistency) of order p if the truncation error for the exact solution is of order $O(\tau^{p+1})$ where $p>0$.

Result 3: A linear N-step method is convergent, i.e., $x_{[t/\tau]}\to x^*(t)$, for all $t\in[0,t_{\mathrm{f}}]$, as $\tau\to 0$, if and only if the method is 0-stable and consistent. That is, 0-stability plus consistency means convergence, which is also known as Dahlquist equivalence theorem.

Result 4: A linear 0-stable consistent method converges with the order of its truncation error.

APPENDIX B

The proof of Theorem 2 is given as follows.

Proof: Based on Taylor expansion [32] with $f_{k+i}=f((k+i)\tau)$, the following equations are derived:

$$f_{k+1}=f(k\tau)+\dot{f}(k\tau)\tau+\frac{\ddot{f}(k\tau)\tau^2}{2!}+\frac{\dddot{f}(k\tau)\tau^3}{3!}+\frac{f^{(4)}(k\tau)\tau^4}{4!}+\frac{f^{(5)}(\xi_1)\tau^5}{5!},\tag{13}$$

$$f_{k-1}=f(k\tau)-\dot{f}(k\tau)\tau+\frac{\ddot{f}(k\tau)\tau^2}{2!}-\frac{\dddot{f}(k\tau)\tau^3}{3!}+\frac{f^{(4)}(k\tau)\tau^4}{4!}-\frac{f^{(5)}(\xi_2)\tau^5}{5!},\tag{14}$$

$$f_{k-2}=f(k\tau)-2\dot{f}(k\tau)\tau+\frac{\ddot{f}(k\tau)(2\tau)^2}{2!}-\frac{\dddot{f}(k\tau)(2\tau)^3}{3!}+\frac{f^{(4)}(k\tau)(2\tau)^4}{4!}-\frac{f^{(5)}(\xi_3)(2\tau)^5}{5!},\tag{15}$$

$$f_{k-3}=f(k\tau)-3\dot{f}(k\tau)\tau+\frac{\ddot{f}(k\tau)(3\tau)^2}{2!}-\frac{\dddot{f}(k\tau)(3\tau)^3}{3!}+\frac{f^{(4)}(k\tau)(3\tau)^4}{4!}-\frac{f^{(5)}(\xi_4)(3\tau)^5}{5!},\tag{16}$$

$$f_{k-4}=f(k\tau)-4\dot{f}(k\tau)\tau+\frac{\ddot{f}(k\tau)(4\tau)^2}{2!}-\frac{\dddot{f}(k\tau)(4\tau)^3}{3!}+\frac{f^{(4)}(k\tau)(4\tau)^4}{4!}-\frac{f^{(5)}(\xi_5)(4\tau)^5}{5!},\tag{17}$$

$$f_{k-5}=f(k\tau)-5\dot{f}(k\tau)\tau+\frac{\ddot{f}(k\tau)(5\tau)^2}{2!}-\frac{\dddot{f}(k\tau)(5\tau)^3}{3!}+\frac{f^{(4)}(k\tau)(5\tau)^4}{4!}-\frac{f^{(5)}(\xi_6)(5\tau)^5}{5!},\tag{18}$$

and

$$f_{k-6}=f(k\tau)-6\dot{f}(k\tau)\tau+\frac{\ddot{f}(k\tau)(6\tau)^2}{2!}-\frac{\dddot{f}(k\tau)(6\tau)^3}{3!}+\frac{f^{(4)}(k\tau)(6\tau)^4}{4!}-\frac{f^{(5)}(\xi_7)(6\tau)^5}{5!},\tag{19}$$

where $\dot{f}$, $\ddot{f}$, $\dddot{f}$, $f^{(4)}$ and $f^{(5)}$ denote the first-order, second-order, third-order, fourth-order and fifth-order derivatives, respectively; ξ_1, ξ_2, ξ_3, ξ_4, ξ_5, ξ_6 and ξ_7 lie in the interval $(k\tau,(k+1)\tau)$, $((k-1)\tau,k\tau)$, $((k-2)\tau,k\tau)$, $((k-3)\tau,k\tau)$, $((k-4)\tau,k\tau)$, $((k-5)\tau,k\tau)$, $((k-6)\tau,k\tau)$ and $((k-7)\tau,k\tau)$, correspondingly; symbol ! denotes the factorial operator. Let (13), (14), (15), (16), (17), (18) and (19) multiply 1, η_1, η_2, η_3, η_4, η_5 and η_6, respectively. Adding them together yields a general discretization formula with six parameters, which is omitted because of the page limitation.

Moreover, to eliminate the terms $\ddot{f}(k\tau)$, $\dddot{f}(k\tau)$ and $f^{(4)}(k\tau)$, we have

$$\begin{cases}1+\eta_1+4\eta_2+9\eta_3+16\eta_4+25\eta_5+36\eta_6=0,\\ 1-\eta_1-8\eta_2-27\eta_3-64\eta_4-125\eta_5-216\eta_6=0,\\ 1+\eta_1+16\eta_2+81\eta_3+256\eta_4+625\eta_5+1296\eta_6=0,\end{cases}$$

that is,

$$\begin{cases}\eta_4=-(21+10\eta_1+24\eta_2+27\eta_3)/16,\\ \eta_5=(35+15\eta_1+32\eta_2+27\eta_3)/25,\\ \eta_6=-(5+2\eta_1+4\eta_2+3\eta_3)/12,\end{cases}$$

and further have

$$\begin{cases}b_0=20/(35-10\eta_1-8\eta_2-3\eta_3),\\ b_1=-(805+970\eta_1+536\eta_2+171\eta_3)/1200.\end{cases}$$

In addition, the characteristic equation of (8) is

$$\varsigma^6+\alpha_1\varsigma^5+\alpha_2\varsigma^4+\alpha_3\varsigma^3+\alpha_4\varsigma^2+\alpha_5\varsigma+\alpha_6=0,$$

where $\alpha_1=(395-970\eta_1-536\eta_2-171\eta_3)/1200$, $\alpha_2=(395+230\eta_1-536\eta_2-171\eta_3)/1200$, $\alpha_3=(395+230\eta_1+664\eta_2-171\eta_3)/1200$, $\alpha_4=(395+230\eta_1+664\eta_2+1029\eta_3)/1200$, $\alpha_5=-(295+130\eta_1+284\eta_2+249\eta_3)/300$ and $\alpha_6=(5+2\eta_1+4\eta_2+3\eta_3)/12$.

By using bilinear transformation [33], [34], i.e., $\varsigma=(\epsilon+1)/(\epsilon-1)$, the following equation is obtained:

$$\varrho_1\epsilon^6+\varrho_2\epsilon^5+\varrho_3\epsilon^4+\varrho_4\epsilon^3+\varrho_5\epsilon^2+\varrho_6\epsilon+\varrho_7=0,$$

where $\varrho_1=525-150\eta_1-120\eta_2-45\eta_3$, $\varrho_2=2625-750\eta_1-600\eta_2-225\eta_3$, $\varrho_3=4900-1400\eta_1-1120\eta_2-420\eta_3$, $\varrho_4=3500-1000\eta_1-800\eta_2-300\eta_3$, $\varrho_5=7455+2670\eta_1+4056\eta_2+2241\eta_3$, $\varrho_6=-525+150\eta_1-1800\eta_2-1875\eta_3$ and $\varrho_7=720+480\eta_1+384\eta_2+624\eta_3$. Then, according to Routh stability criterion [33], [34], (7) is finally obtained. The proof is thus completed. ■

REFERENCES

[1] B. Fernandez, P. J. Herrera, and J. A. Cerrada, "A simplified optimal path following controller for an agricultural skid-steering robot," *IEEE Access*, vol. 7, pp. 95932–95940, 2019.

[2] W. Li and R. Xiong, "Dynamical obstacle avoidance of task-constrained mobile manipulation using model predictive control," *IEEE Access*, vol. 7, pp. 88301–88311, 2019.

[3] L. Cheng, M. Chen, and Z. Li, "Design and control of a wearable hand rehabilitation robot," *IEEE Access*, vol. 6, pp. 74039–74050, 2018.

[4] X. Tan, C.-B. Chng, Y. Su, K.-B. Lim, and C.-K. Chui, "Robot-assisted training in laparoscopy using deep reinforcement learning," *IEEE Robot. Autom. Lett.*, vol. 4, no. 2, pp. 485–492, Apr. 2019.

[5] S. Fahmi, C. Mastalli, M. Focchi, and C. Semini, "Passive whole-body control for quadruped robots: Experimental validation over challenging Terrain," *IEEE Robot. Autom. Lett.*, vol. 4, no. 3, pp. 2553–2560, Jul. 2019.
[6] S. Thabit and A. Mohades, "Multi-robot path planning based on multi-objective particle swarm optimization," *IEEE Access*, vol. 7, pp. 2138–2147, 2018.
[7] D. Guo, F. Xu, and L. Yan, "New pseudoinverse-based path-planning scheme with PID characteristic for redundant robot manipulators in the presence of noise," *IEEE Trans. Control Syst. Technol.*, vol. 26, no. 6, pp. 2008–2019, Nov. 2018.
[8] A. Atawnih, D. Papageorgiou, and Z. Doulgeri, "Kinematic control of redundant robots with guaranteed joint limit avoidance," *Robot. Auto. Syst.*, vol. 79, pp. 122–131, May 2016.
[9] Z. Tan, Y. Hu, L. Xiao, and K. Chen, "Robustness analysis and robotic application of combined function activated RNN for time-varying matrix pseudo inversion," *IEEE Access*, vol. 7, pp. 33434–33440, 2019.
[10] Z. Li, F. Xu, Q. Feng, J. Cai, and D. Guo, "The application of ZFD formula to kinematic control of redundant robot manipulators with guaranteed motion precision," *IEEE Access*, vol. 6, pp. 64777–64783, 2018.
[11] A. De Luca, L. Lanari, and G. Oriolo, "Control of redundant robots on cyclic trajectories," in *Proc. IEEE Int. Conf. Robot. Automat.*, vol. 1, May 1992, pp. 500–506.
[12] D. Guo and Y. Zhang, "Li-function activated ZNN with finite-time convergence applied to redundant-manipulator kinematic control via time-varying Jacobian matrix pseudoinversion," *Appl. Soft Comput.*, vol. 24, pp. 158–168, Nov. 2014.
[13] Z. Zhang and Z. Yan, "Hybrid-level joint-drift-free scheme of redundant robot manipulators synthesized by a varying-parameter recurrent neural network," *IEEE Access*, vol. 6, pp. 34967–34975, 2018.
[14] Z. Zhang, S. Chen, and S. Li, "Compatible convex–nonconvex constrained qp-based dual neural networks for motion planning of redundant robot manipulators," *IEEE Trans. Control Syst. Technol.*, vol. 27, no. 3, pp. 1250–1258, May 2019.
[15] L. Jin, S. Li, J. Yu, and J. He, "Robot manipulator control using neural networks: A survey," *Neurocomputing*, vol. 285, pp. 23–34, Apr. 2018.
[16] L. Jin, S. Li, H. Wang, and Z. Zhang, "Nonconvex projection activated zeroing neurodynamic models for time-varying matrix pseudoinversion with accelerated finite-time convergence," *Appl. Soft Comput.*, vol. 62, pp. 840–850, Jan. 2018.
[17] J. Luo, X. Yu, Y. Yin, H. Tan, and Y. Zhang, "Acceleration-level Z2G0 controller for redundant manipulator end-effector tracking," in *Proc. 11th Int. Conf. Fuzzy Syst. Knowl. Discovery (FSKD)*, vol. 1, Aug. 2014, pp. 860–865.
[18] L. Xiao, B. Liao, S. Li, Z. Zhang, L. Ding, and L. Jin, "Design and analysis of FTZNN applied to the real-time solution of a nonstationary Lyapunov equation and tracking control of a wheeled mobile manipulator," *IEEE Trans. Ind. Informat.*, vol. 14, no. 1, pp. 98–105, Jan. 2018.
[19] J. Chen and Y. Zhang, "Continuous and discrete zeroing neural dynamics handling future unknown-transpose matrix inequality as well as scalar inequality of linear class," *Numer. Algorithms*, pp. 1–19, Mar. 2019. doi: 10.1007/s11075-019-00692-z.
[20] L. Xiao, "A nonlinearly-activated neurodynamic model and its finite-time solution to equality-constrained quadratic optimization with nonstationary coefficients," *Appl. Soft Comput.*, vol. 40, pp. 252–259, Mar. 2016.
[21] L. Jin, Y. Zhang, and B. Qiu, "Neural network-based discrete-time Z-type model of high accuracy in noisy environments for solving dynamic system of linear equations," *Neural Comput. Appl.*, vol. 29, no. 11, pp. 1217–1232, Jun. 2018.
[22] Z. Zhang, Y. Lu, L. Zheng, S. Li, Z. Yu, and Y. Li, "A new varying-parameter convergent-differential neural-network for solving time-varying convex QP problem constrained by linear-equality," *IEEE Trans. Autom. Control*, vol. 63, no. 12, pp. 4110–4125, Dec. 2018.
[23] L. Jin and Y. Zhang, "Discrete-time Zhang neural network of $O(\tau^3)$ pattern for time-varying matrix pseudoinversion with application to manipulator motion generation," *Neurocomputing*, vol. 142, pp. 165–173, Oct. 2014.
[24] D. Guo, Z. Nie, and L. Yan, "Novel discrete-time Zhang neural network for time-varying matrix inversion," *IEEE Trans. Syst., Man, Cybern., Syst.*, vol. 47, no. 8, pp. 2301–2310, Aug. 2017.
[25] L. Xiao and Y. Zhang, "Acceleration-level repetitive motion planning and its experimental verification on a six-link planar robot manipulator," *IEEE Trans. Control Syst. Technol.*, vol. 21, no. 3, pp. 906–914, May 2013.
[26] Y. Zhang, H. Wu, Z. Zhang, L. Xiao, and D. Guo, "Acceleration-level repetitive motion planning of redundant planar robots solved by a simplified LVI-based primal-dual neural network," *Robot. Comput.-Integr. Manuf.*, vol. 29, no. 2, pp. 328–343, Apr. 2013.
[27] S. Boyd and L. Vandenberghe, *Convex Optimization*. Cambridge, U.K.: Cambridge Univ. Press, 2004.
[28] J. Nocedal and S. J. Wright, *Numerical Optimization*. New York, NY, USA: Springer, 1999.
[29] E. Shli and D. F. Mayers, *An Introduction to Numerical Analysis*. Cambridge, U.K.: Cambridge Univ. Press, 2003.
[30] Y. Zhang and Z. Zhang, *Repetitive Motion Planning and Control of Redundant Robot Manipulators*. London, U.K.: Springer, 2013.
[31] D. F. Griffiths and D. J. Higham, *Numerical Methods for Ordinary Differential Equations: Initial Value Problems*. London, U.K.: Springer, 2010.
[32] J. H. Mathews and K. D. Fink, *Numerical Methods Using MATLAB*. Englewood Cliffs, NJ, USA: Prentice-Hall, 2004.
[33] A. V. Oppenheim, *Discrete-Time Signal Processing*, 3rd ed. Upper Saddle River, NJ, USA: Pearson Higher Education, 2010.
[34] K. Ogata, *Modern Control Engineering*, 4th ed. Englewood Cliffs, NJ, USA: Prentice-Hall, 2001.

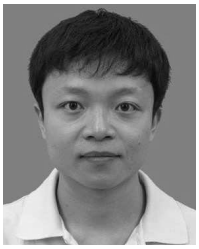

JIANRONG CHEN received the B.S. degree in engineering management from Guangzhou University, Guangzhou, China, in 2005, and the M.S. degree in computer application technology from Guangxi University for Nationalities, Nanning, China, in 2009. He is currently pursuing the Ph.D. degree in computer science and technology with the School of Data and Computer Science, Sun Yat-sen University, Guangzhou. He is also an Assistant Researcher with the Information and Education Technology Center, Youjiang Medical University for Nationalities, Baise, China. His main research interests include robotics, neural networks, numerical computation, and intelligent optimization.

YUNONG ZHANG (S'02–M'03) received the B.S. degree in industrial electrical automation from the Huazhong University of Science and Technology, Wuhan, China, in 1996, the M.S. degree in control theory and control engineering from the South China University of Technology, Guangzhou, China, in 1999, and the Ph.D. degree in mechanical and automation engineering from The Chinese University of Hong Kong, Hong Kong, in 2003. He is currently a Professor with the School of Data and Computer Science, Sun Yat-sen University, Guangzhou. Before joining Sun Yat-sen University in 2006, he has been with the National University of Singapore, the University of Strathclyde, and the National University of Ireland at Maynooth, since 2003. His main research interests include robotics, neural networks, computation, and optimization. More information is available at http://sdcs.sysu.edu.cn/content/2477.